Universitat de Girona
Escola Politècnica Superior

Treball final de grau

Estudi: Grau en Tecnologies Industrials

Títol:

A RESEARCH ON CONCRETE FRACTURE MECHANICS.
TESTING AND ANALYZING THE FRACTURE ENERGY OF CONCRETE.

Document: Resum de l'Estudi

Alumne: Santiago Rodríguez Lorente

Tutor: Cristina Barris Peña

Departament: Enginyeria Mecànica i de la Construcció Industrial

Àrea: Enginyeria de la Construcció i de Mecànica dels Medis Continus i Teoria d'Estructures

Convocatòria (mes/any): Juny/2016

A RESEARCH ON CONCRETE FRACTURE MECHANICS

TESTING AND ANALYZING THE FRACTURE ENERGY OF CONCRETE

ABSTRACT

This research is focused on finding the fracture energy of concrete G_F at common environmental conditions for different concrete mixtures, trying to see how G_F changes while the composition or the properties of concrete change. For achieving this goal, first, the fracture mechanisms that rule concrete fracture will be reviewed, together with the recommended testing procedures. After that, different series of concrete are tested and G_F is determined for them. Finally, the registered G_F is compared for all series, trying to find a connection between the composition and the properties of concrete with G_F, if this is possible with the available data. If not, more tests should be done in the future for this research.

NOTATION

A – Far tail constant	D – Depth	G_f –Size-dependent fracture energy	OX – X-axis	W_f – Recorded fracture work
a – Notch depth	f_c– Compressive strength	g_f – Local fracture energy	P – Load	w_G – Gravity center
a_1 – Transition zone depth	FPZ – Fracture Process Zone	h – Knifes thickness	P_1 – Corrected load	W_{tail} – Tail work
$Agg.$ – Aggregate	f_t – Axial tensile strength	L – Length	S – Span length	α – Notch to depth ratio
B – Width	g – Gravity field force	m – Mass	w – Crack width	δ – Displacement
$CMOD$ – Crack Mouth Opening Displacement	G_F – Real specific fracture energy	N – Notch width	W/C – Ratio water/cement	ε – Strain
			w_c – Critical crack width	σ – Normal stress

1 INTRODUCTION

1.1 BACKGROUND

One of the most important materials in civil engineering is concrete, fact that makes really important to know its behavior. The classic failure criteria for brittle materials can give certain information[1], but this might not be realistic, because of what is called the *size effect*, where the failure criteria are valid for relative small structures, but not for the large ones[2,3].

An energy-based theory was proposed[4] and, recently, one of the resulting theories applicable to concrete emerged[5–8], which are the concrete fracture mechanics and the cohesive law. The main parameters are a material independent-only fracture energy G_F and a softening function $\sigma - w$ for the stress at the damaged regions from the matrix[9]. G_F was difficult to confirm as a material property because of the *size effect*, but after studying it and proposing correction methods to the tests, G_F was confirmed to be a material size-independent property[10–14].

1.2 PURPOSE

The aim of this paper is to study G_F at common environmental conditions for different concrete mixtures with different mechanical properties and composition.

1.3 SCOPE

To achieve it, the following proceed is proposed.

First, a search of the state of the art will be done. After that, the test proposed by the recommendations will be reproduced seeking stability. Then, a continuous testing of different concretes will be performed, beginning with low- and normal-strength concretes. While this is happening, and if it is possible, other alternative methods will be used to check the current methodology. Finally, G_F will be found and, if there is enough data, its variability will be checked.

2 QUASI-BRITTLE MATERIALS FRACTURE MECHANICS FUNDAMENTALS

2.1 THE COHESIVE CRACK MODEL

The applicable energy based fracture theory to concrete is the *fictitious* or *cohesive crack model*. It is based on changing how to measure the matrix degradation, due to microcracking and microdislocations, which cancels the stress concentration at the crack tip and weakens the capability of transferring stresses[6–9,15].

This zone of reduced stresses is called the *Fracture Process Zone* (*FPZ*) and it has a certain width and depth that moves at the top of the real crack tip. The *FPZ* is governed by the microcracking displacements, which can be computed as real crack width w, even though any visible crack can be seen (see Figure 1).

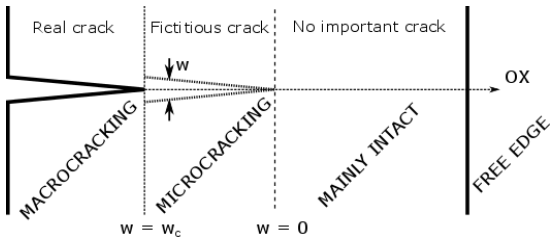

Figure 1: Real and fictitious crack tip and crack development front

2.2 THE SOFTENING PHENOMENON AND THE FRACTURE ENERGY

The displacements of the non-visible cracked region show how damaged the matrix is and they are used to compute the stress that the material at the *FPZ* region is able to transfer. These stresses define the softening function $\sigma - w$.

The softening is caused by the weaken ability of the material damaged core to transfer stresses, because of microcracking, which cause internal fissures, reducing the surface and its strength. The softening occurs in the *FPZ*, where the maximum stress is located at the most internal point and reaches the axial tensile strength f_t, because the degradation causes the stress concentration to disappear, and the minimum strength is determined by the $\sigma - w$ function, where the real crack appears when the critical crack width w_c is achieved and no stress is capable to be transferred and there is not any contact from now on between the two new surfaces (see Figure 2).

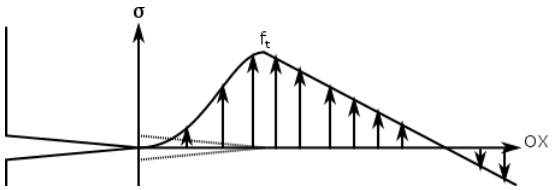

Figure 2: Stress distribution at an advanced fracture point

The softening function defines the second part of the constitutive equation that characterizes the concrete behavior. The first part is when the material is not cracked, neither micro- or macro-scale, where the classic stress versus strain σ - ε curve governs. Once the w becomes higher and f_t is achieved, $\sigma - w$ curve (Figure 3) is now of application until w arrives at w_c. At this point, stress is zero (see Figure 1 to find these zones).

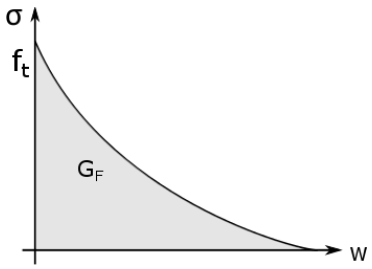

Figure 3: A stress vs. crack opening curve applicable to concrete

The area enclosed down the softening function is the real fracture energy G_F (Equation 1).

$$G_F = \int_0^{+\infty} \sigma(w)dw = \int_0^{w_c} \sigma(w)dw \qquad (1)$$

2.3 LOCAL FRACTURE MODEL

This theory wants to propose a different treatment for the energy release at the end of the fracture process (the same as the correction methods), which brings associated an explanation for the size effect. This model proposes an energy distribution over the specimen cross section, called the local energy g_f, which is the maximum possible at the initial stages, with a value similar to G_F, and a reduction while the crack progresses[16,17].

This reduction at the last stages is because the finite dimensions of the *FPZ*, which has a certain maximum depth and width. As the crack progresses and the *FPZ* at its front, this zone approaches the boundary. In the *FPZ* exists the cohesive stresses, so, a reduction of its dimensions will cause less area for these stresses to act. When the boundary is near, in what is called the transition zone, whose depth is a_1, and the *FPZ* is unable to get its maximum depth, but lower, the energy required to create the same amount of free surfaces is reduced.

This means that the complete division of a specimen and the calculation of the energy required give a mean value lower than the G_F, which is the size-dependent fracture energy G_f. An example of the approximation for this model is given at Figure 4. This procedure and theory have been proved valid for the G_F determination[18].

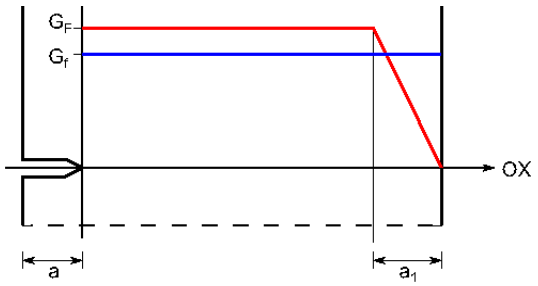

Figure 4: Local fracture energy distribution and its mean value

3 THE TEST AND PROCEDURES

3.1 EXPERIMENTAL PROCEDURES AND TESTS

The reasonable test would be a direct axial tensile test, but this is unfeasible to perform on concrete. So, the test applied will be the three-point bend test (Figure 5), based on the recommended procedures and corrections[19,20], accepting possible execution limitations on specimens, control systems or machinery and trying to solve them.

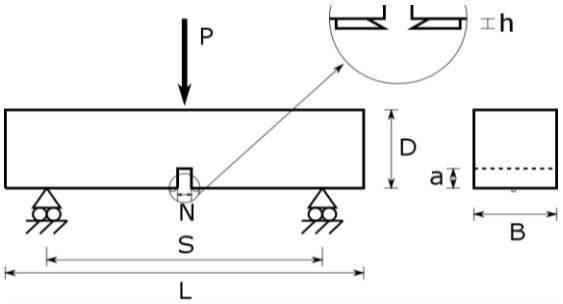

Figure 5: Main dimensions of a three-point bend test set up

The specimens will have a notch at its center in order to create a single crack with a load introduced vertically at its center with a load head and cell in order to record the force and the head displacement. At the notch mouth, a clip gage will be placed in order to record the Crack Mouth Opening Displacement *CMOD*. The fracture energy, in this case is the size-dependent G_f, is given at Equation 2.

$$G_f = \frac{1}{B(D-a)}\left(\int_0^{\delta_u} P\, d\delta + mg\delta_u\right) \qquad (2)$$

Where *B, D* and *a* are sizes, *P* the load, δ_u the total displacement, *g* the gravity force of 9.81N/kg and *m* is the specimen mass, to use only if the self-weight is not corrected with a double length specimen. If it is, *m* is zero.

3.2 LOAD VS. DISPLACEMENT TAIL CORRECTION

This correction method is based on the behavior of the tail of the test, extracted by a theoretical approximation of two bodies joined by the cohesive stresses only at the final stage[12] and further developed[21]. The essentials are:

1. The $P - \delta$ and $P - w$ curves are cut at $CMOD \leq 4D/300$ and corrected load P_1 is used by setting the last load to zero
2. The fracture work is the area enclosed up this cut zone
3. The last part of the $P - w$ curve is taken under the 5% of the new peak load and the *CMOD* values are used to create an artificial variable *X*, whose use is to fit Equation 3
4. *A* is the far tail constant, which is used to add a new work, called the tail work W_{tail}, computed with Equation 4.

$$P_1 = X(A + KX) = AX + KX^2 \quad (3)$$

$$W_{tail} = 2A\delta_u^{-1} \quad (4)$$

The addition of this tail work divided by the cross section *B(D-a)* to G_f give us the real fracture energy G_F.

The most modern proposed correction method gives also the chance to create the bilinear approximation of the softening curve, because *A* is related to the gravity center w_G of the area enclosed down the $\sigma - w$ curve.

Note: further details and equations at Chapter 3.3 or ref.[21]

3.3 FRACTURE ENERGY BY MEANS OF THE LOCAL FRACTURE ENERGY THEORY

Based on the local fracture energy, Equation 5 can be found and it is the way to obtain G_F. α is the notch to depth ratio. For its good use, two series of the same concrete mixture have to be cast, one with short notches and another with long notches and the *S* has to be 4 or more times *D* for a maximum aggregate size 10mm or 7 or more times *D* until a maximum aggregate size of 20mm[22].

$$G_f(\alpha) = \begin{cases} G_F \cdot \left(1 - \dfrac{a_1}{2D(1-\alpha)}\right) & if\ D - a > a_1 \\ G_F \cdot \dfrac{(1-\alpha)D}{2a_1} & if\ D - a \leq a_1 \end{cases} \quad (5)$$

Then, one calculates G_f with Equation 2 for two different notch depths and entering them into Equation 5 and solving it, G_F and a_1 are found for a concrete mixture.

4 MATERIALS

The different tested campaigns are given now through their mechanical properties at Table 1 and their composition at Table 2. The main procedure is the $P - \delta$ tail correction, because it gives more information and statistical variables are available. For the 29I2016B series the procedure of local fracture energy is used in order to check the currently used methodology.

The specimens are usually sized with 100mm depth *D*, 100mm width *B*, 600mm length *L*, 300mm span *S* and notches between 29 to 31mm of depth *a*. 29I2016B series has notches of 10mm approx. and 42mm approx. for the short and long notch series.

The campaigns have a chronological name and a second one, type *X-S/A/C/W*, with the cement type *I* for I 52.5R and *II* for II 32.5N/B-L; *S*, *A* and *C* for the percentage in sand, aggregate and cement and *W* for the *w/c* without the integer part, which is always zero.

Table 1: Mechanical properties from the tested campaign

CAMPAIGN	2ND NAME	f_t (MPa)	f_c (MPa)
23X2015	*II-42/47/11/87*	0.78	6.43 (0.34)
14XII2015	*I-XX/XX/14/45*	2.45 (0.53)	17.03*
29I2016	*II-40/45/15/67*	1.42 (0.23)	11.43* (2.28)
10III2016	*II-44/44/11/86*	1.09 (0.05)	9.27
17III2016	*II-39/50/11/82*	1.69 (0.07)	13.87
01IV2016	*II-43/43/14/77*	1.26 (0.02)	12.53
07IV2016	*II-38/48/14/77*	1.44 (0.07)	15.37
14IV2016	*II-43/43/14/65*	2.13 (0.17)	20.36
21IV2016	*II-38/48/14/65*	1.31	16.32

Table 2: Composition from the tested campaigns

CAMPAIGN	Sand 0-2	Agg. 5-10	II/B-L 32.5N	W/C
23X2015	42.35%	47.05%	10.60%	0.867
14XII2015	HA-25/F/15/IIa Max. Agg. Size 15mm		(I 52.5R) 275kg/m^3	0.450
29I2016A	40.00%	45.00%	15.00%	0.674
29I2016B	40.00%	45.00%	15.00%	0.667
10III2016	44.34%	44.34%	11.32%	0.859
17III2016	38.95%	49.90%	11.15%	0.818
01IV2016	43.14%	43.14%	13.72%	0.770
07IV2016	38.15%	48.13%	13.72%	0.770
14IV2016	43.14%	43.14%	13.72%	0.650
21IV2016	38.15%	48.13%	13.72%	0.650

Note: all these details, test setup, mechanical properties and furthermore can be seen at Project's Chapter 4

5 RESULTS AND DISCUSSION

The most important results are given at Table 3.

Table 3: Results for G_F and other parameters for the tested campaigns

CAMPAIGN	G_F (J/m^2)	w_c (μm)	W_{tail}/W_f
23X2015	81.9 (11.6)	723.5	57.96%
14XII2015	146.1 (35.6)	172.6	10.56%
29I2016A	145.9 (23.4)	450.7	25.65%
29I2016B	154.4	a_1 = 50.48mm	
10III2016	93.4 (22.3)	516.6	41.34%
17III2016	155.9 (17.9)	445.8	33.51%
01IV2016	134.7 (8.5)	378.9	26.06%
07IV2016	164.3 (10.1)	479.7	30.42%
14IV2016	214.2 (23.2)	349.8	22.92%
21IV2016	145.8 (34.7)	469.0	30.59%

These results were obtained after applying the tail correction to 44 three-point bending tests, where the $P - \delta$ and the $P - w$ curves were recorded. An example is given at Figure 6 and Figure 7. The softening curve bilinear approximation is also found, alongside with a possible and valid global reduced bilinear approximation (see Figure 8).

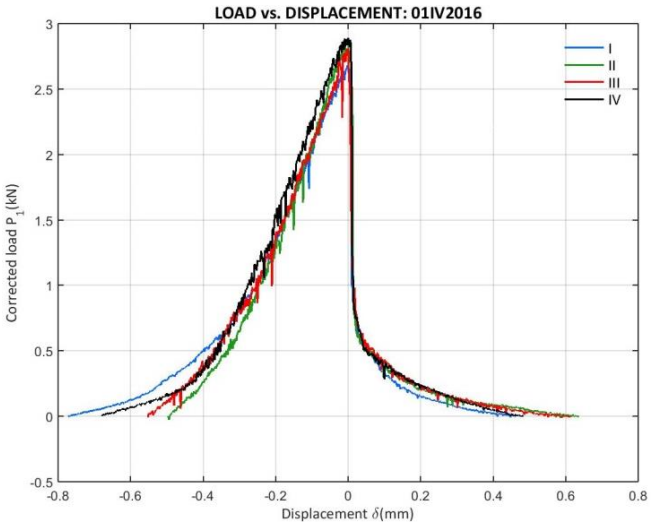

Figure 6: Corrected load vs. Displacement for the 01IV2016 campaign

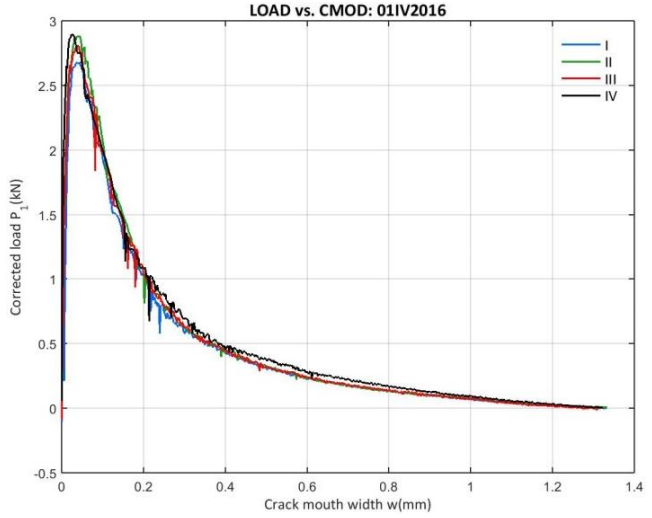

Figure 7: Corrected load vs. *CMOD* for the 01IV2016 campaign

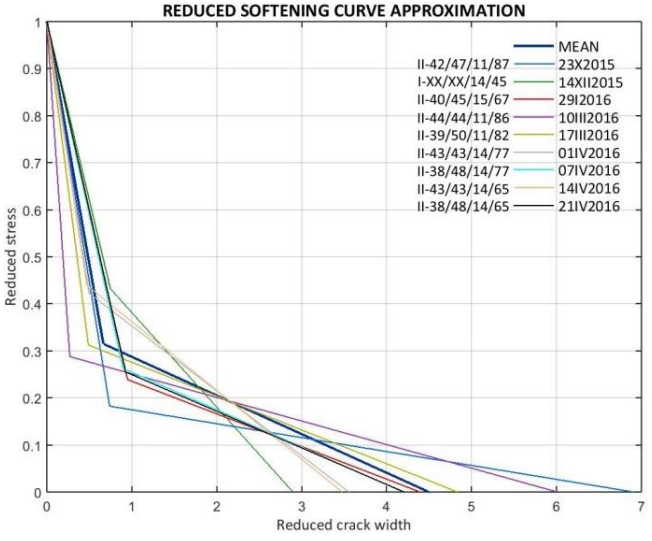

Figure 8: Reduced form of the softening curve bilinear approximation

It is time to check now the possible connections of G_F with some of the parameters of interest. These have been found for the sand proportion and for *w/c* (Figure 9) in form of an inverse relation between them and G_F, although few campaigns do not show this behavior, and for the cement content (Figure 10) and the properties f_c (Figure 11) and f_t (Figure 12) in terms of a direct relation between them and G_F. For the aggregate content, it is difficult to see any kind of bound and, for the maximum aggregate size, the experimentation has not been enough.

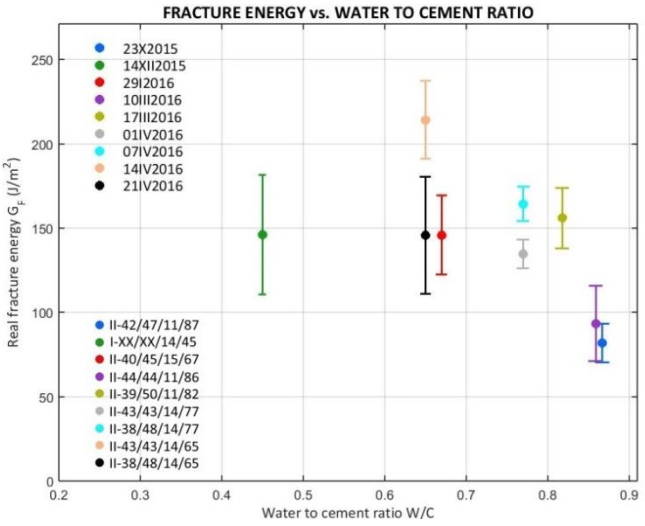

Figure 9: Fracture energy vs. Water to cement ratio

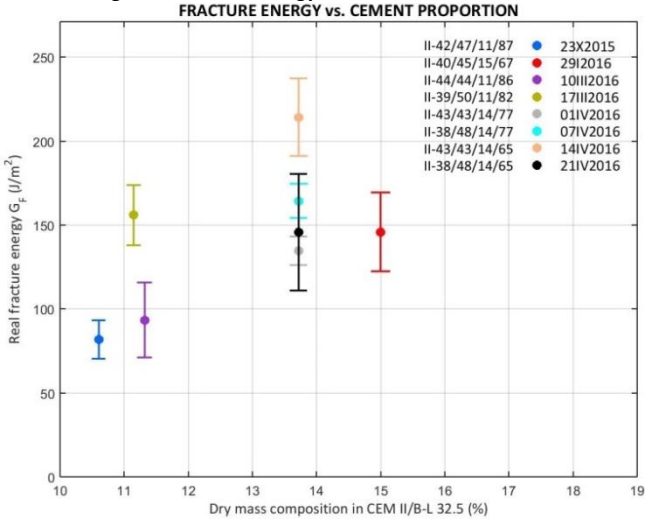

Figure 10: Fracture energy vs. Cement II/B-L 32.5N proportion

The lack of experimentation, the existence of some contradictive events with the statements done and the fact that the registered load values show a cyclical behavior at the loading and unloading stages of the test with a possible energy loss due to hysteresis (*see Chapter 5.1.2 for further information*) make impossible to create a predictive model valid at any case and everywhere, because there is a possibility that the predictive model would be only valid for our testing systems and machines and difficulties to have a proper fitting. For this reason, this has not been done.

Note: more figures and results at Chapter 5 of the project.

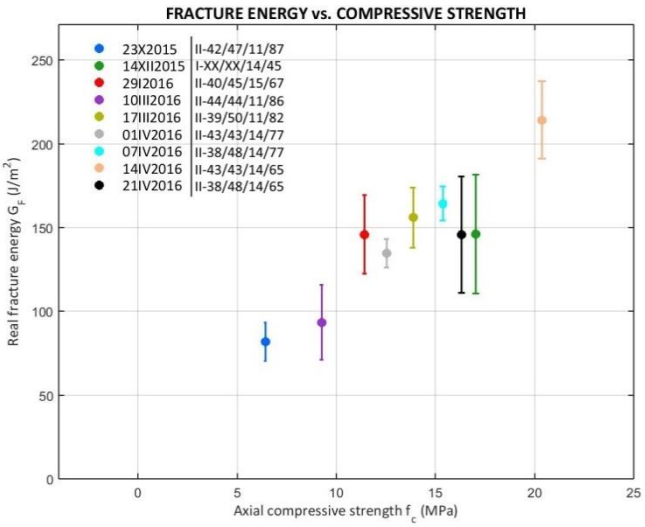

Figure 11: Fracture energy vs. Compressive strength

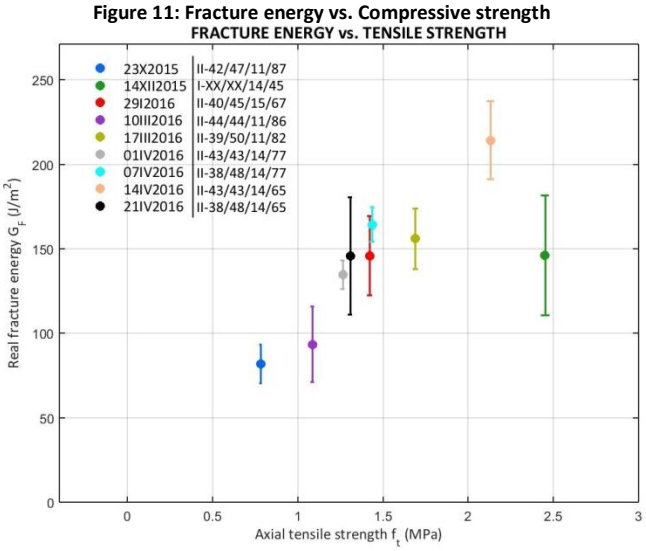

Figure 12: Fracture energy vs. Tensile strength

6 CONCLUSIONS

The mechanisms of concrete fracture have been reviewed and also the commonly used testing procedures for the determination of G_F. A total of forty-seven three-point bending tests, twenty-one Brazilian tests and eleven direct compression tests have been carried out for this project.

The fracture energy of concrete has been analyzed with the variation of some parameters and some clear connections have been detected, although others with more difficulties.

For this reason and other commented at Chapter 5, in order to enhance the study possibilities at this field of research, an improvement of the testing system and procedures, which have been applied at this project, must be done.

After this, this research can be continued with a wider experimental field for finding more valid and comparable with the work of other researchers G_F values for more concrete mixtures at environmental conditions and then a more correct and precise predictive model can be built, using the composition or properties as parameters.

Further work can be done after adding more parameters to this predictive model, such as the environmental conditions, the age of concrete, the speed of the loading situation, the type of actions or the type of sand, aggregate or cement. Also, the effect of fatigue can be studied for this.

7 REFERENCES

1. William, K. J. & Warnke, E. P. Constitutive model for the triaxial behavior of concrete. (1975).
2. Bažant, Z. P. Size effect in blunt fracture: concrete, rock, metal. *Journal of Engineering Mechanics* (1984).
3. Bažant, Z. P., Ozbolt, J. & Eligehausen, R. Fracture size effect: review of evidence for concrete structures. *Journal of structural engineering* **120,** 2377–2398 (1994).
4. Griffith, A. A. The phenomena of rupture and flow in solids. *Philosophical Transactions of the Royal Society of London. Series A, Containing Papers of a Mathematical or Physical Character* 163–198 (1921).
5. Bažant, Z. P. Concrete fracture models: testing and practice. *Engineering fracture mechanics* **69,** 165–205 (2002).
6. Hillerborg, A., Modéer, M. & Petersson, P.-E. Analysis of crack formation and crack growth in concrete by means of fracture mechanics and finite elements. *Cement and concrete research* **6,** 773–781 (1976).
7. Modéer, M. A fracture mechanics approach to failure analyses of concrete materials. (Lund University, 1979).
8. Barenblatt, G. The formation of equilibrium cracks during brittle fracture. General ideas and hypotheses. Axially-symmetric cracks. *Journal of Applied Mathematics and Mechanics* **23,** 622–636 (1959).
9. Bažant, Z. P. & Planas, J. *Fracture and size effect in concrete and other quasibrittle materials*. **16,** (CRC press, 1997).
10. Guinea, G. V, Planas, J. & Elices, M. Measurement of the fracture energy using three-point bend tests: Part 1—Influence of experimental procedures. *Materials and Structures* **25,** 212–218 (1992).
11. Planas, J., Elices, M. & Guinea, G. V. Measurement of the fracture energy using three-point bend tests: Part 2—Influence of bulk energy dissipation. *Materials and Structures* **25,** 305–312 (1992).
12. Elices, M., Guinea, G. V & Planas, J. Measurement of the fracture energy using three-point bend tests: Part 3—Influence of cutting the P-δ tail. *Materials and Structures* **25,** 327–334 (1992).
13. Bažant, Z. P. & Kazemi, M. T. Size dependence of concrete fracture energy determined by RILEM work-of-fracture method. *International Journal of Fracture* **51,** 121–138 (1991).
14. Gustafsson, P.-J. Fracture mechanics studies of non-yielding materials like concrete: modelling of tensile fracture and applied strength analyses. (Lund University, 1985).
15. Petersson, P.-E. Crack growth and development of fracture zones in plain concrete and similar materials. (Lund University, 1981).
16. Hu, X. Size effects in toughness induced by crack close to free edge. *AEDIFICATIO Publishers, Fracture Mechanics of Concrete Structures,* **3,** 2011–2020 (1998).
17. Duan, K., Hu, X. & Wittmann, F. H. Boundary effect on concrete fracture and non-constant fracture energy distribution. *Engineering Fracture Mechanics* **70,** 2257–2268 (2003).
18. Abdalla, H. M. & Karihaloo, B. L. Determination of size-independent specific fracture energy of concrete from three-point bend and wedge splitting tests. *Magazine of concrete research* **55,** 133–141 (2003).
19. RILEM 50-FMC. Determination of the Fracture Energy of Mortar and Concrete by Means of Three-Point Bend Tests on Notched Beames. Draft Recommendation. *Materials and Structures* **18,** 285–290 (1985).
20. ACI COMMITTEE 446. ASTM Test procedure: Fracture toughness testing of concrete. 72 (2010).
21. Fathy, A. M., Sanz, B., Sancho, J. M. & Planas, J. Determination of the bilinear stress-crack opening curve for normal-and high-strength concrete. *Fatigue & Fracture of Engineering Materials & Structures* **31,** 539–548 (2008).
22. Karihaloo, B. L., Abdalla, H. M. & Imjai, T. A simple method for determining the true specific fracture energy of concrete. *Magazine of concrete research* **55,** 471–481 (2003).

The author:

Santiago Rodríguez Lorente

Girona, Monday 13th June 2016